Supporting Information for

Two discrete dimeric metal-chalcogenide supertetrahedral clusters

Jin Wu,[†] Ning Chen,[†] and Tao Wu[*,†,‡]

† College of Chemistry, Chemical Engineering and Materials Science, Soochow University, Suzhou, Jiangsu 215123, China.

‡ College of Chemistry and Materials Science, Guangdong Provincial Key Laboratory of Functional Supramolecular Coordination Materials and Applications, Jinan University, Guangzhou, 510632.

Experimental Sections

General Details. All reagents and solvents employed in these synthetic studies were purchased from commercial and used without further purification. Indium powder (In, 99.99%), sulfur powder (S, 99.5%), (*R*)-(-)-2-amino-1-butanol, (2-AB, $C_4H_{11}NO$, 98%), 1,5-diazabicyclo[4.3.0]non-5-ene (DBN, $C_7H_{12}N_2$, 99%), 2,6-dimethylpyridine (2,6-DMPy, C_7H_9N, 99.5%), and 3,5-dimethylpiperidine (3,5-DMPr, $C_7H_{15}N$, 99.5%).

Synthesis of ISC-29 (T3-m). Indium powder (114 mg, 1.00 mmol) and sulfur powder (96 mg, 3.00 mmol) were mixed with DBN (1 mL, 8.17 mmol), 2,6-DMPy (0.8 mL, 20.62 mmol), 2-AB (2 mL, 21.50 mmol) were mixed in a 25 mL Teflon lining stainless steel and stirred for 30 min, then heated to 180 ℃ for 7 days. After cooling to room temperature, colorless block crystals were obtained with a yield of 16.6% based on In composition.

Synthesis of ISC-30 (T3-d). Indium powder (114 mg, 1.00 mmol) and sulfur powder (160 mg, 5.00 mmol) were mixed with DBN (1 mL, 8.17 mmol), 2,6-DMPy (3 mL, 77.32 mmol), 2-AB (1 mL, 10.75 mmol) were mixed in a 25 mL Teflon lining stainless steel and stirred for 30 min, then heated to 200 ℃ for 7 days. After cooling to room temperature, colorless block crystals along with some impurities were obtained with a yield of 5.3% based on In. Impurities can be removed manually under a microscope from crystal samples after ultrasonic washing and drying with ethanol. The phase purity was identified by powder X-ray diffraction measurements.

Synthesis of ISC-31 (P1-d). Indium powder (114 mg, 1.00 mmol) and sulfur powder (96 mg, 3.00 mmol) were mixed with 3,5-DMPr (2.5 mL, 25.27 mmol) were mixed in a 25 mL Teflon lining stainless steel and stirred for 30 min, then heated to 190 ℃ for 7 days. After cooling to room temperature, rhombohedral transparent crystals were obtained with a yield of 15.8% based on In. A small amount of colorless flaky crystals were obtained by ultrasonication in ethanol. The phase purity was identified by powder X-ray diffraction measurements.

Single-Crystal X-ray Diffraction Characterization. The single-crystal X-ray diffraction measurements on **ISC-29, ISC-30, ISC-31** were performed on a Bruker Smart CPAD area diffractometer with nitrogen-flow temperature controller using graphite-monochromated MoKα (λ= 0.71073 Å) radiation at 120 K. The structure was solved by direct method using SHELXS2014 and the refinement against all reflections of the compound was performed using OLEX2.

Powder X-ray Diffraction (PXRD) Characterization. PXRD data were collected on a desktop

diffractometer (D2 PHASER, Bruker, Germany) using Cu-Kα (λ=1.54056 A) radiation operated at 30 kV and 10 mA. The samples were ground into fine powders for several minutes before the test.

Elemental Analysis. Energy dispersive spectroscopy (EDS) analysis was performed on scanning electron microscope (SEM) equipped with energy dispersive spectroscopy (EDS) detector. An accelerating voltage of 25 kV and 40 s accumulation time were applied.

Thermogravimetric (TG) Measurement. A Shimadzu TGA-50 thermal analyzer was used to measure the TG curve by heating the sample from room temperature to 800℃ with heating rate of 10 ℃/min under N_2 flow.

Fourier-Transform Infrared Absorption. Fourier transform-Infrared spectral analysis was performed on a Thermo Nicolet Avatar 6700 FT-IR spectrometer with cesium iodide optics allowing the instrument to observe from 600-4000 cm^{-1}.

UV-Vis Absorption. Room-temperature solid-state UV-Vis diffusion reflectance spectra of **ISC-29, 30, 31** was measured on a SHIMADZU UV-3600 UV-Vis-NIR spectrophotometer coupled with an integrating sphere by using BaSO4 powder as the reflectance reference. The absorption spectra were calculated from reflectance spectra by using the Kubelka-Munk function: $F(R) = \alpha/S = (1-R)^2/2R$, where R, α, and S are the reflection, the absorption and the scattering coefficient, respectively. In order to determine the band edge of the direct-gap semiconductor, the relation between the absorption coefficients (α) and the incident photon energy ($h\nu$) is exhibited as $\alpha h\nu = A(h\nu - E_g)^{1/2}$, where A is a constant that relates to the effective masses associated with the valence and conduction bands, and E_g is the optical transition gap of the solid material. The band gap of the obtained samples can be determined from the Tauc plot with $[F(R) * h\upsilon]^2$ vs. $h\upsilon$ by extrapolating the linear region to the abscissa.

^{1}H NMR characterization. Proton nuclear magnetic resonance (^{1}H NMR) spectra were recorded using a Bruker instrument (400 MHz) and internally referenced to tetramethylsilane or residual solvent signals. The crystals picked out from the mother liquor were cleaned with weighing paper to remove the solvent molecules on the crystal surface and used directly for the NMR analysis. The corresponding signal could be detected by using d^6-dimethyl sulfoxide (DMSO) as a solvent.

Table. S1 Crystal data and structure refinement parameters for **ISC-29~31**.

Compound Name	**ISC-29**	**ISC-30**	**ISC-31**
Cluster formula	$In_{10}S_{20}$	$In_{20}S_{39}$	$In_{16}S_{33}$
Formula weight	1789.5	3546.74	2894.41
Crystal system	monoclinic	monoclinic	trigonal
Space group	*C*2/*c*	$P2_1/n$	*R*-3
a/Å	20.8083(9)	22.2852(10)	24.9718(18)
b/Å	20.6445(8)	15.5779(8)	24.9718(18)
c/Å	19.7748(8)	46.388(2)	21.679(2)
α/°	90	90	90
β/°	98.3600(10)	97.9400(10)	90
γ/°	90	90	120
Volume/$Å^3$	8404.5(6)	15949.3(13)	11708(2)
ρ_{calc}/g·cm^{-3}	2.911	1.477	1.815
μ/mm^{-1}	5.778	3.344	2.792
Reflections collected	43727	154489	18848
GOF on F^2	1.047	1.030	1.030
R_1, wR_2 ($I>2\sigma(I)$)	0.0541, 0.1524	0.0710, 0.1733	0.0551, 0.1311
R_1, wR_2 (*all data*)	0.0976, 0.1999	0.1151, 0.1988	0.0754, 0.1511

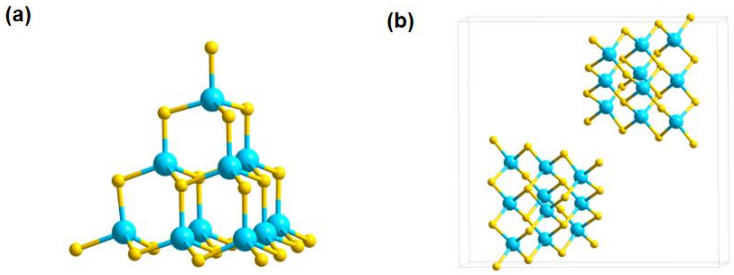

Fig. S1. (a) Structure of the T3 cluster in **ISC-29**; (b) view of the unit cell of **ISC-29**.

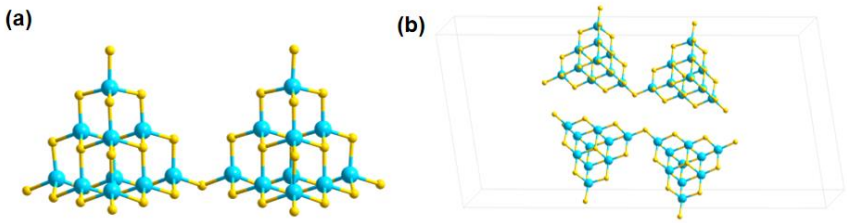

Fig. S2. (a) Molecular structure of the cluster anion in **ISC-30**; (b) view of the unit cell of **ISC-30**.

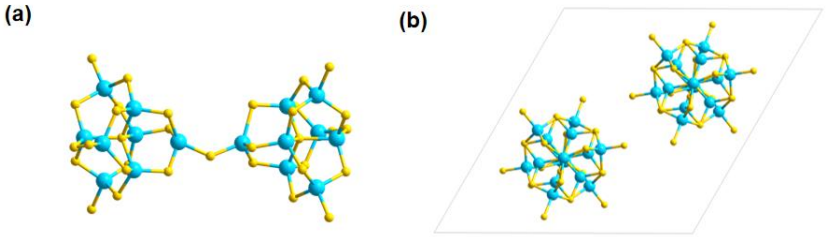

Fig. S3. (a) Molecular structure of the cluster anion in **ISC-31**; (b) view of the unit cell of **ISC-31**.

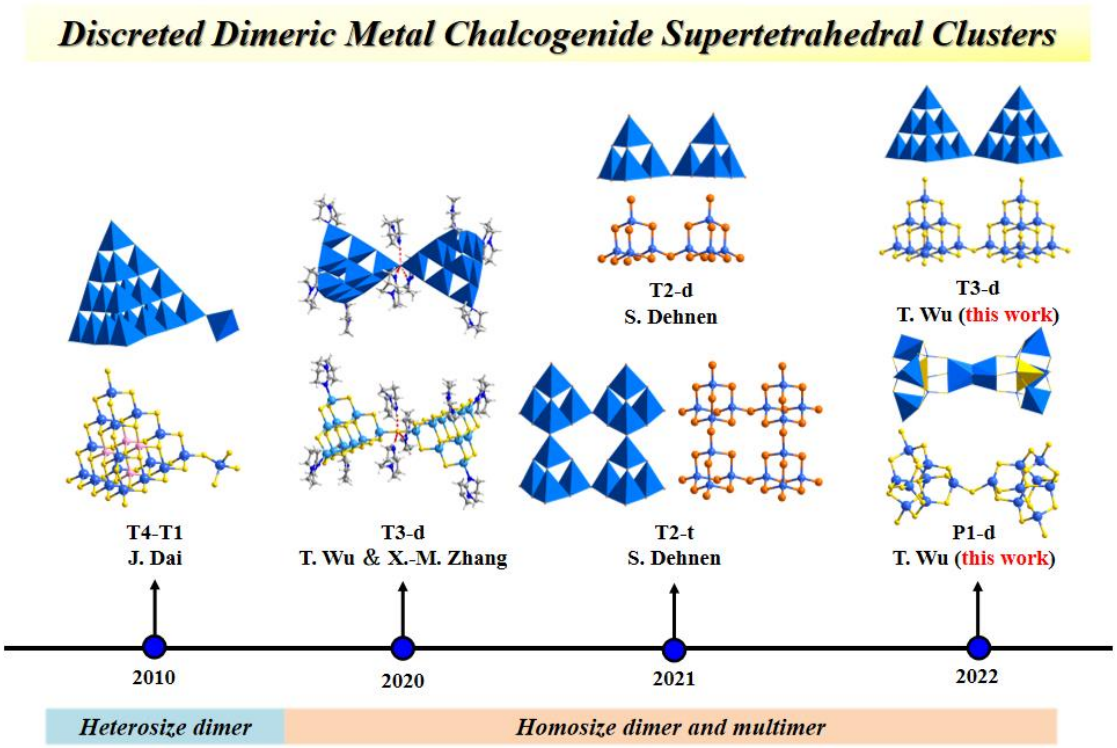

Fig. S4. Summary of the existing discrete dimers and multimer of metal-chalcogenide supertetrahedral clusters.

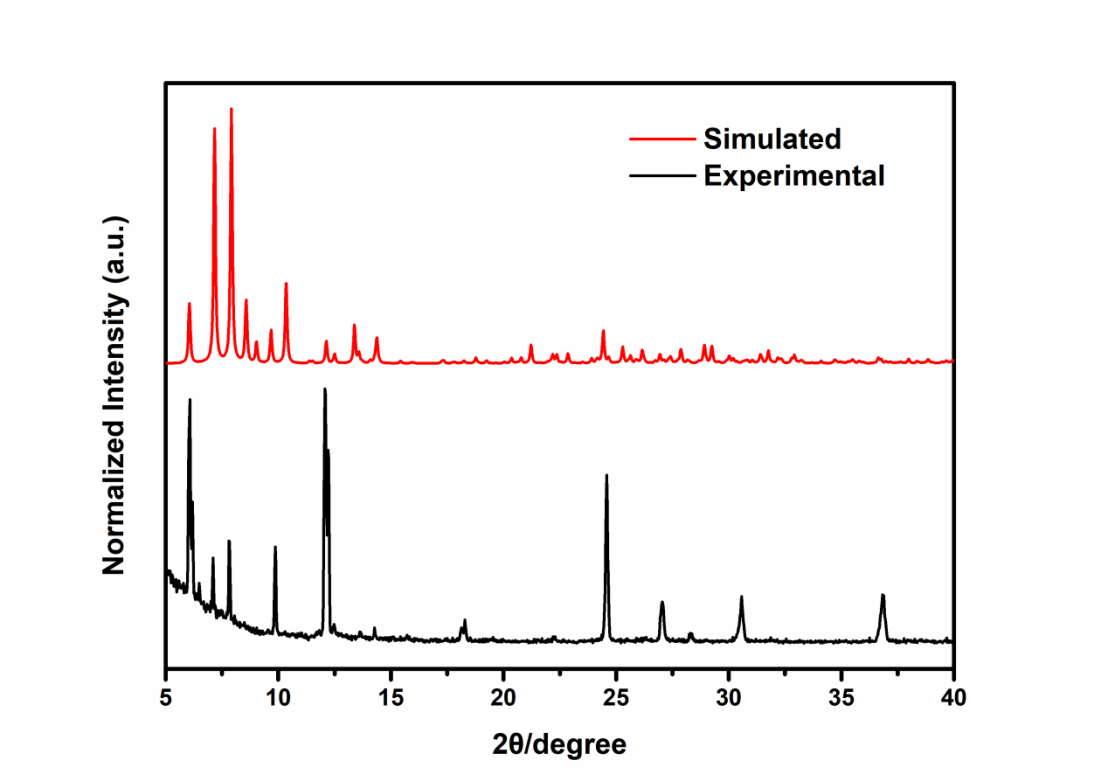

Fig. S5. Powder X-ray diffraction (PXRD) pattern of as-synthesized **ISC-29** and its simulated one.

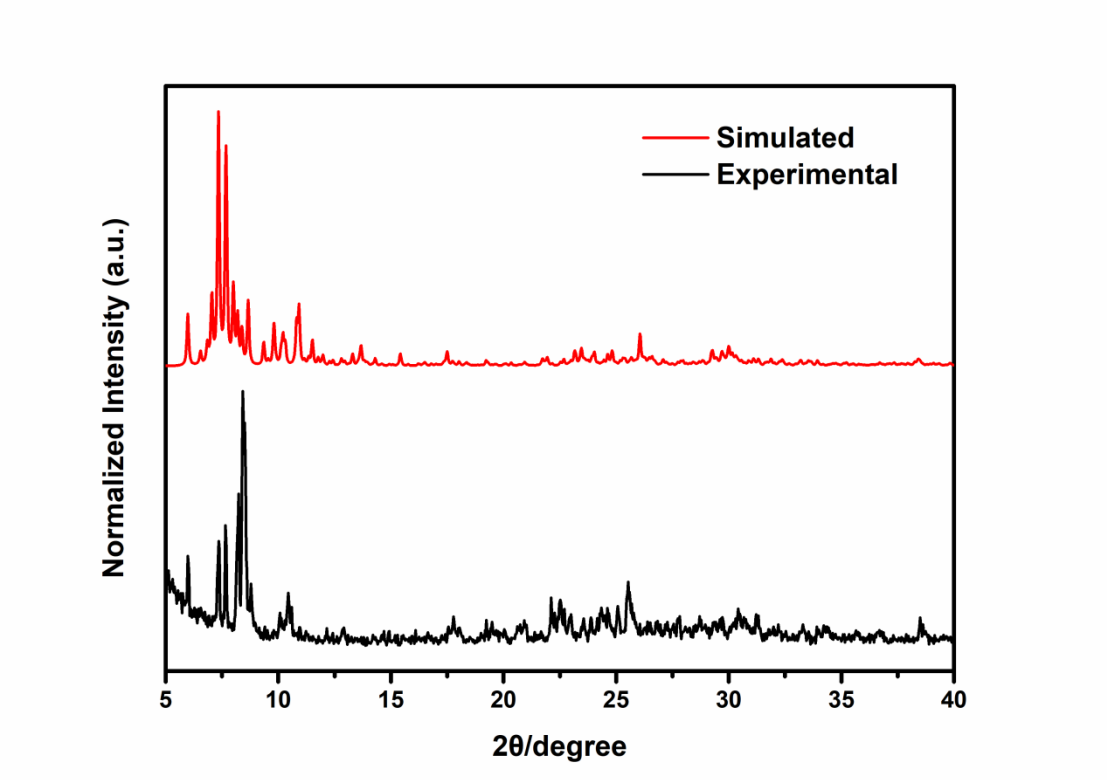

Fig. S6. Powder X-ray diffraction (PXRD) pattern of as-synthesized **ISC-30** and its simulated one.

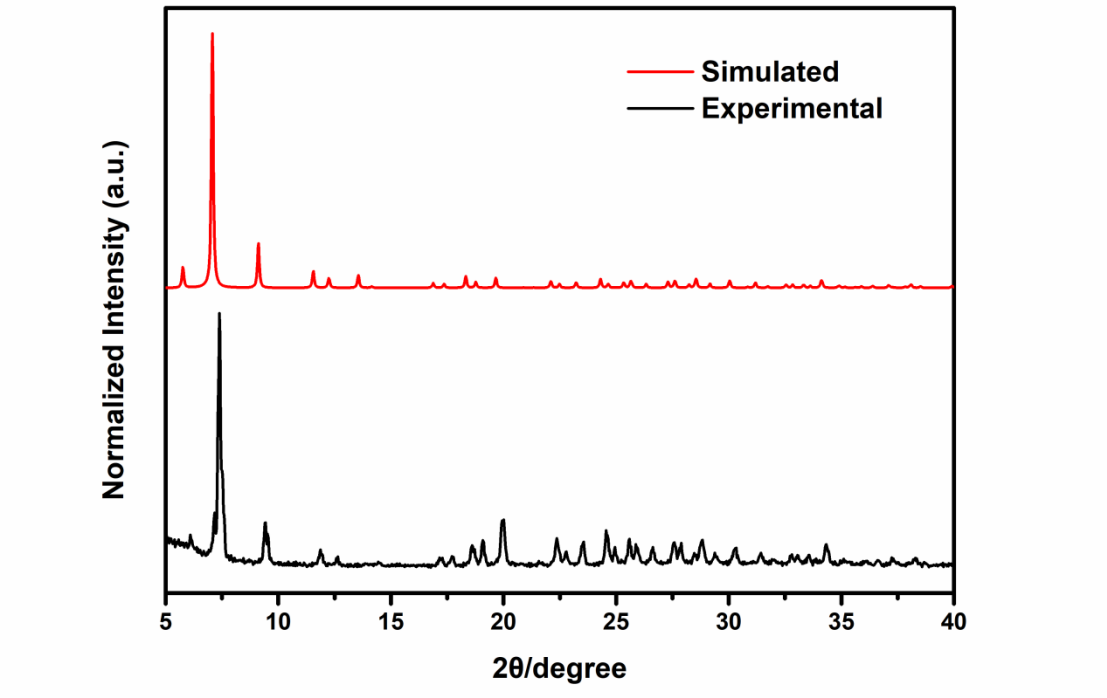

Fig. S7. Powder X-ray diffraction (PXRD) pattern of as-synthesized **ISC-31** and its simulated one.

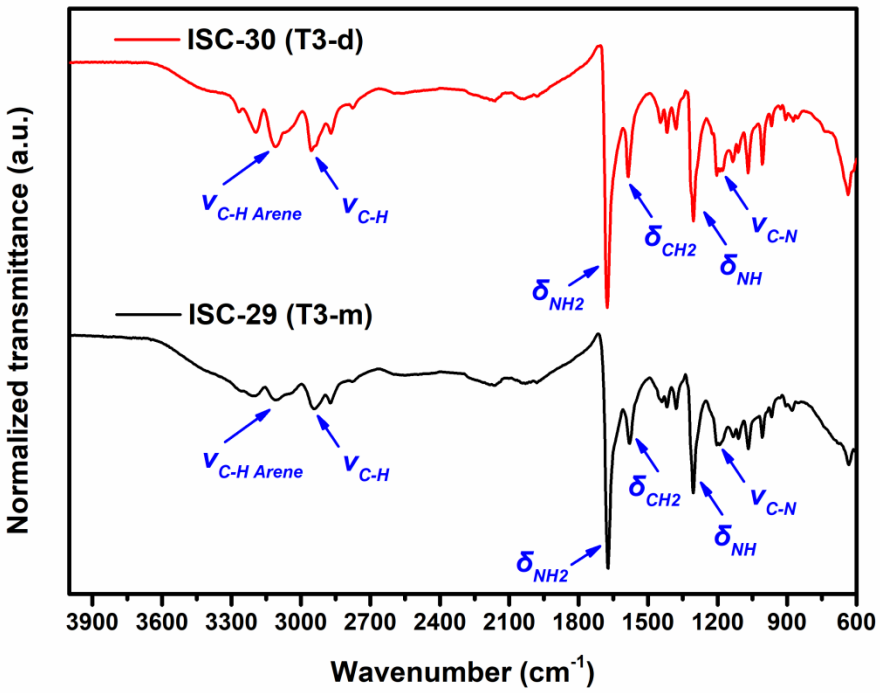

Fig. S8. FT-IR spectra for **ISC-29** and **ISC-30**.

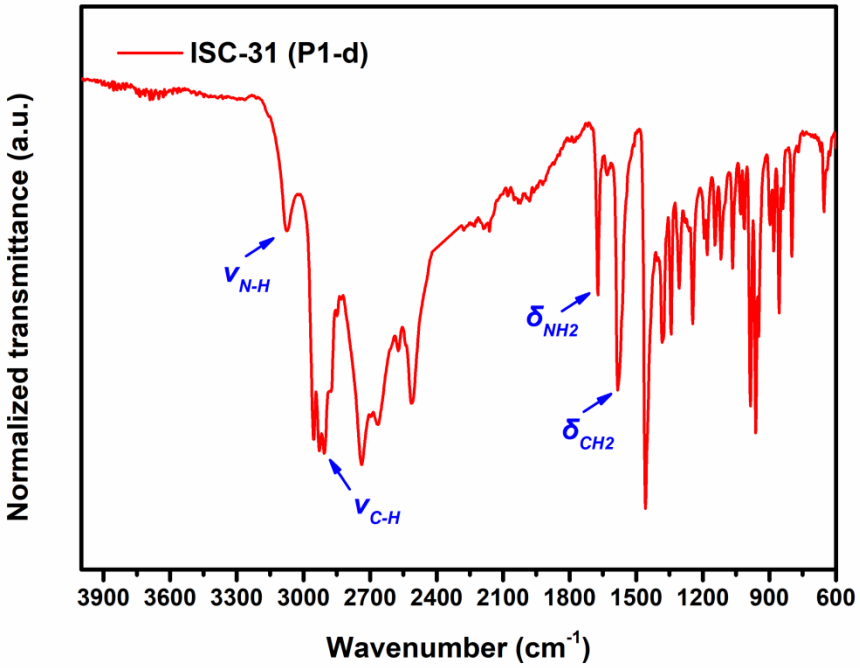

Fig. S9. FT-IR spectrum for **ISC-31**.

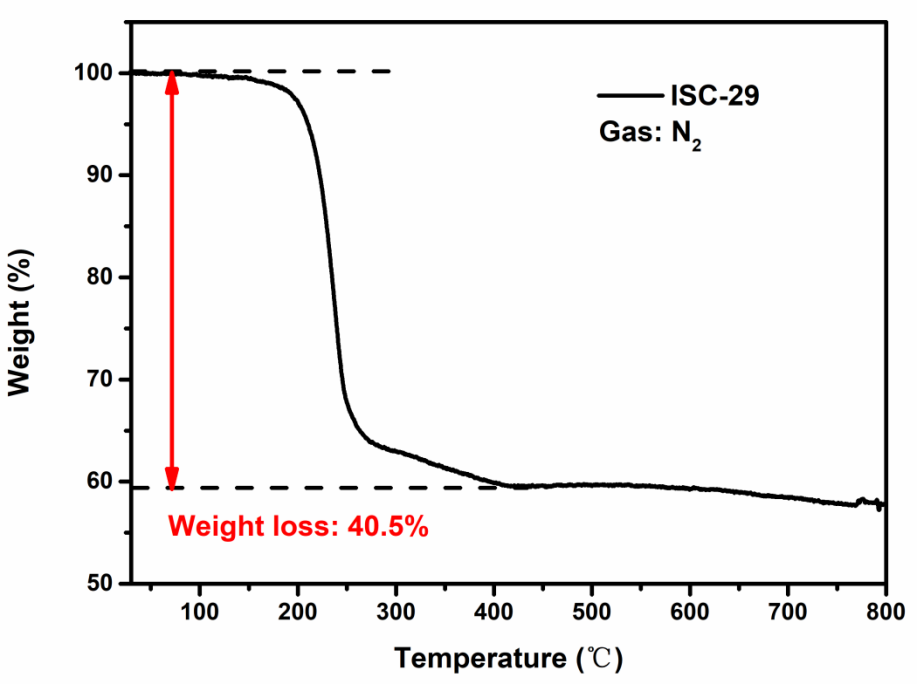

Fig. S10. TGA curve of **ISC-29**. **ISC-29** undergoes the total step weight loss about 40.5% from room temperature to 400℃, which is in good agreement with the calculated value from the SCXRD analysis, corresponding to the loss of the organic components (Calcd. 41.16%).

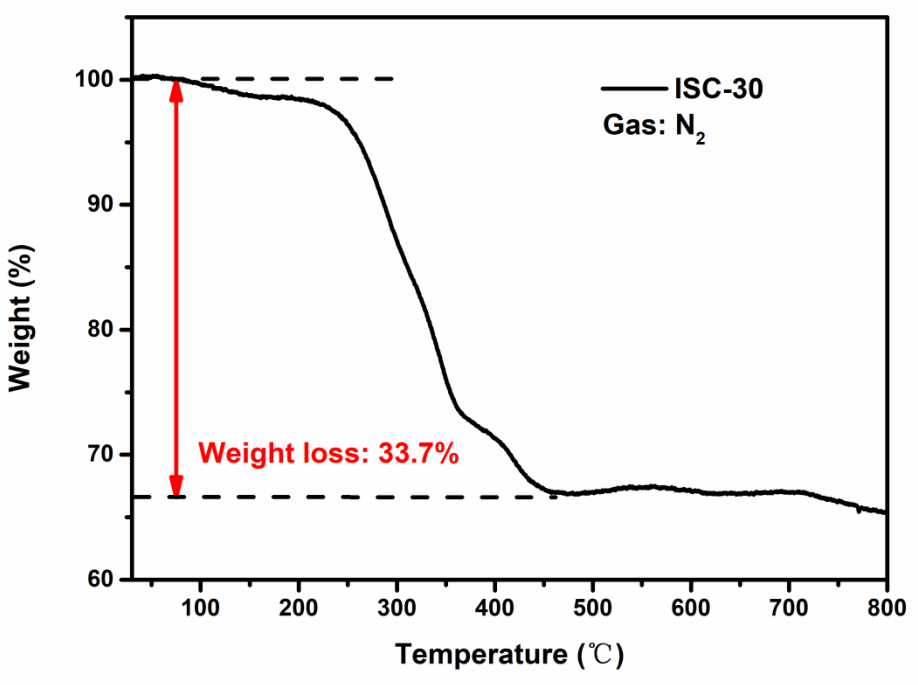

Fig. S11. TGA curve of **ISC-30**. **ISC-30** undergoes the total step weight loss about 33.7% from room temperature to 460 ℃, which is in good agreement with the calculated value from the SCXRD analysis, corresponding to the loss of the organic components (Calcd. 34.01%).

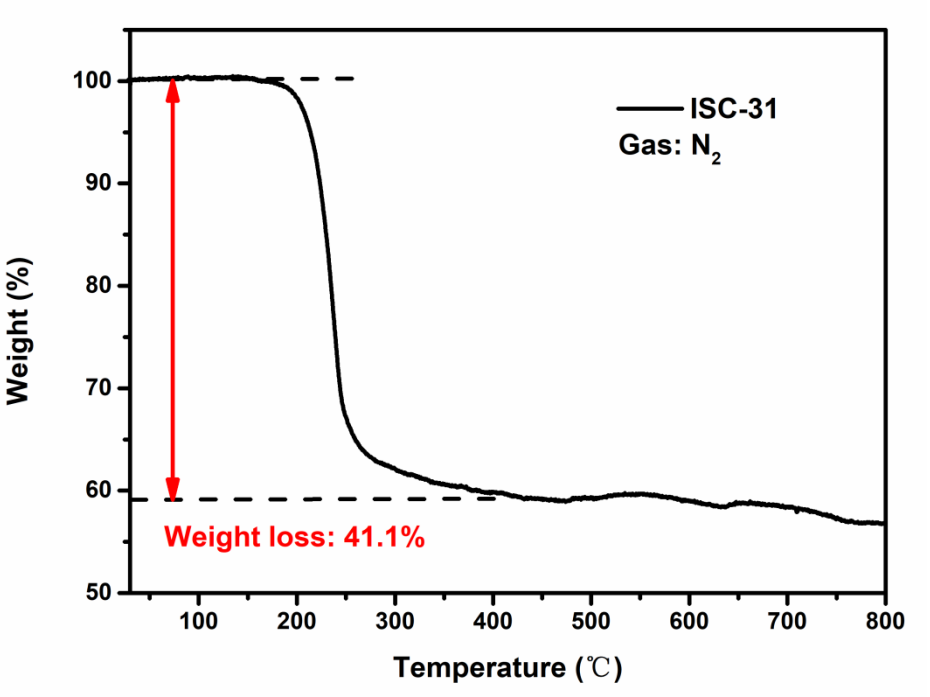

Fig. S12. TGA curve of **ISC-31**. **ISC-31** undergoes the total step weight loss about 41.1% from room temperature to 450℃, which is in good agreement with the calculated value from the SCXRD analysis, corresponding to the loss of the organic components (Calcd. 41.5%).

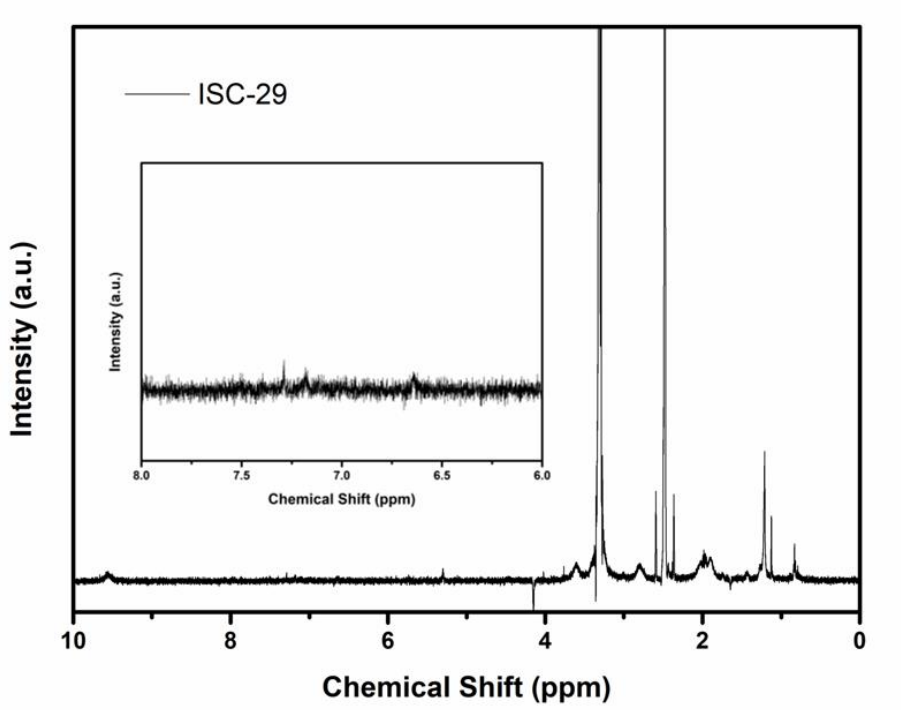

Fig. S13. ^{1}H-NMR spectrum of **ISC-29.** The inset shows the high-resolution signals between chemical shift 6-8, suggesting that there are no 2,6-DMPy in the composition of crystalline **ISC-29**. The signals at 2.5 ppm and 3.3 ppm belong to solvent d^6-DMSO and H_2O, respectively.

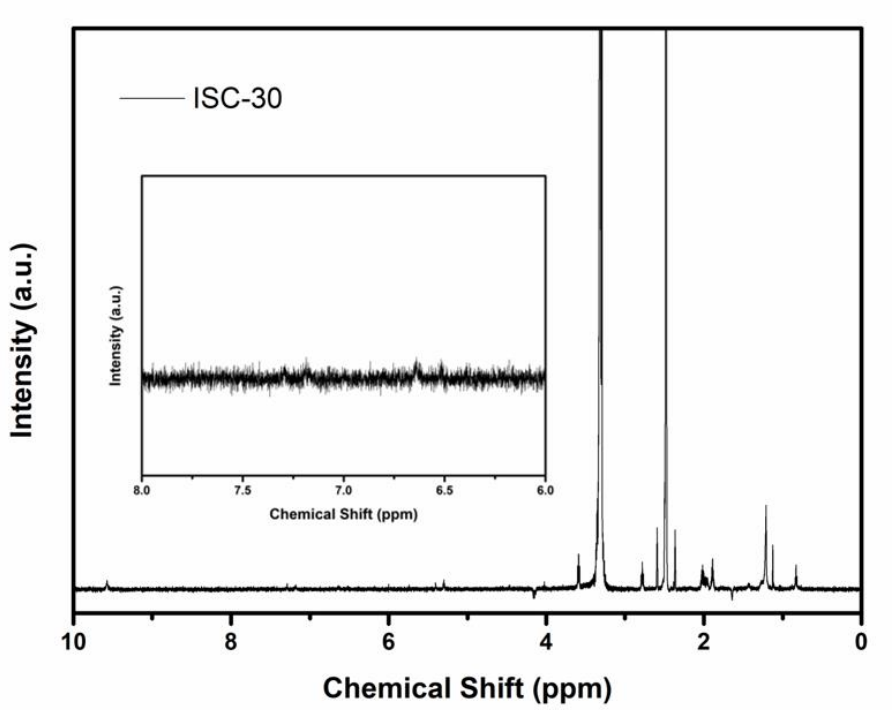

Fig. S14. [1]H-NMR spectrum of **ISC-30.** The inset shows was high-resolution signals between chemical shift 6-8, suggesting that there are no 2,6-DMPy in the composition of crystalline **ISC-30**. The signals at 2.5 ppm and 3.3 ppm belong to solvent d^6-DMSO and H_2O, respectively.

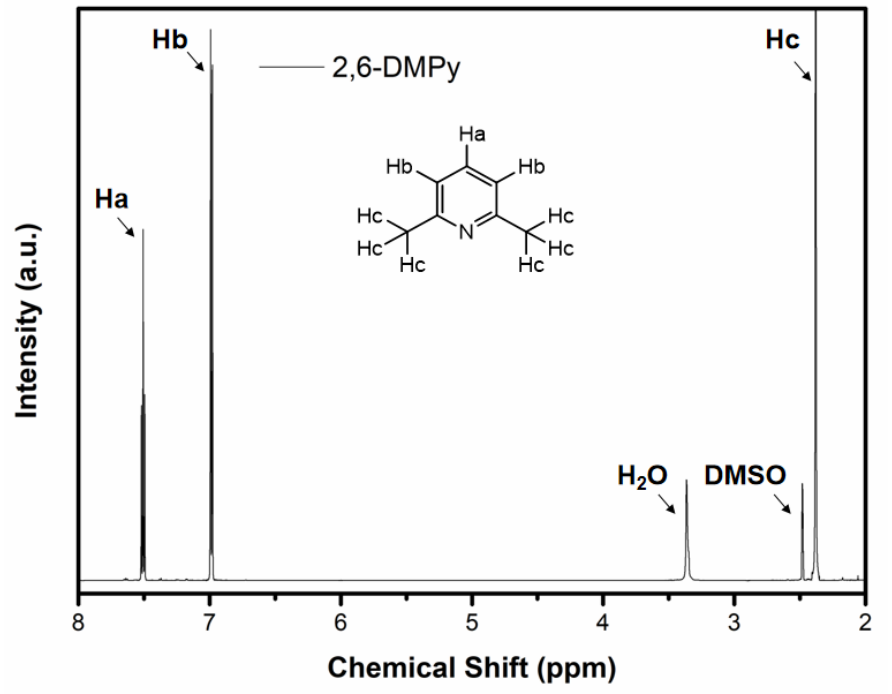

Fig. S15. [1]H-NMR spectrum of 2,6-DMPy. The signals at 2.5 ppm and 3.3 ppm belong to solvent d^6-DMSO and H_2O, respectively.

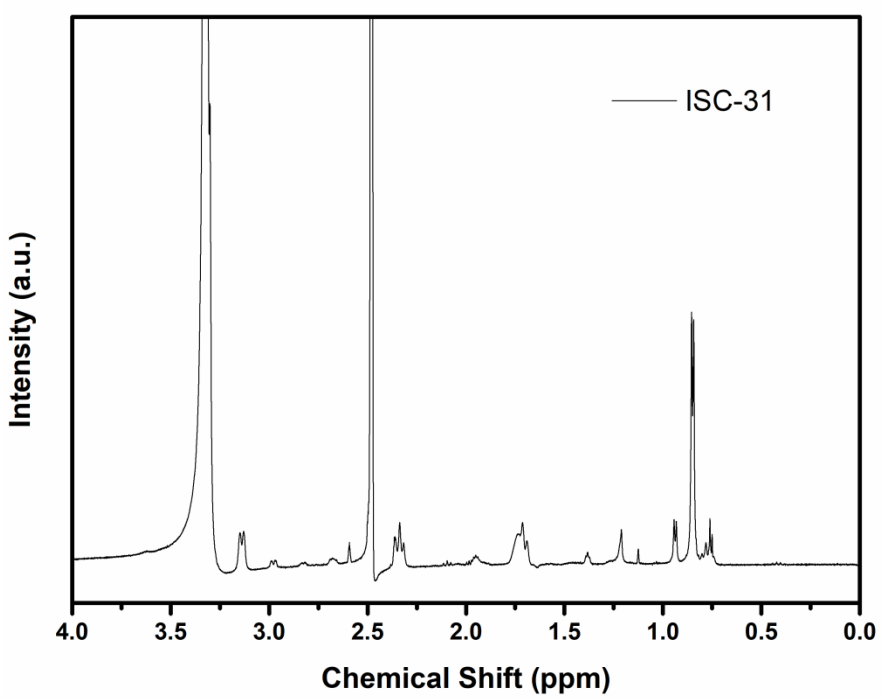

Fig. S16. ^{1}H-NMR spectrum of **ISC-31**. The signals at 2.5 ppm and 3.3 ppm belong to solvent d^{6}-DMSO and H_2O, respectively.

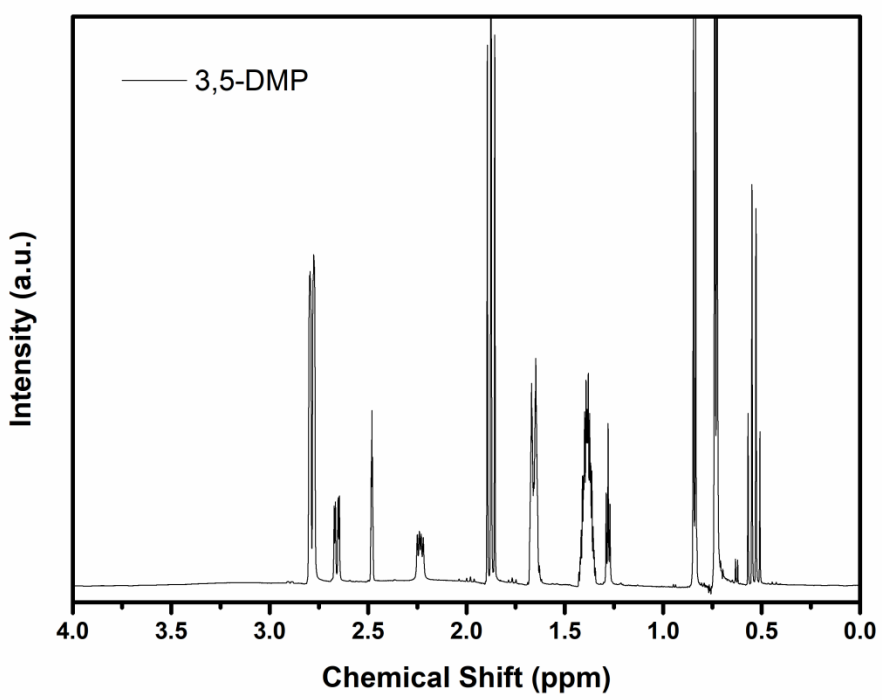

Fig. S17. ^{1}H-NMR spectrum of 3,5-DMPr. The signals at 2.5 ppm and 3.3 ppm belong to solvent d^{6}-DMSO and H_2O, respectively.

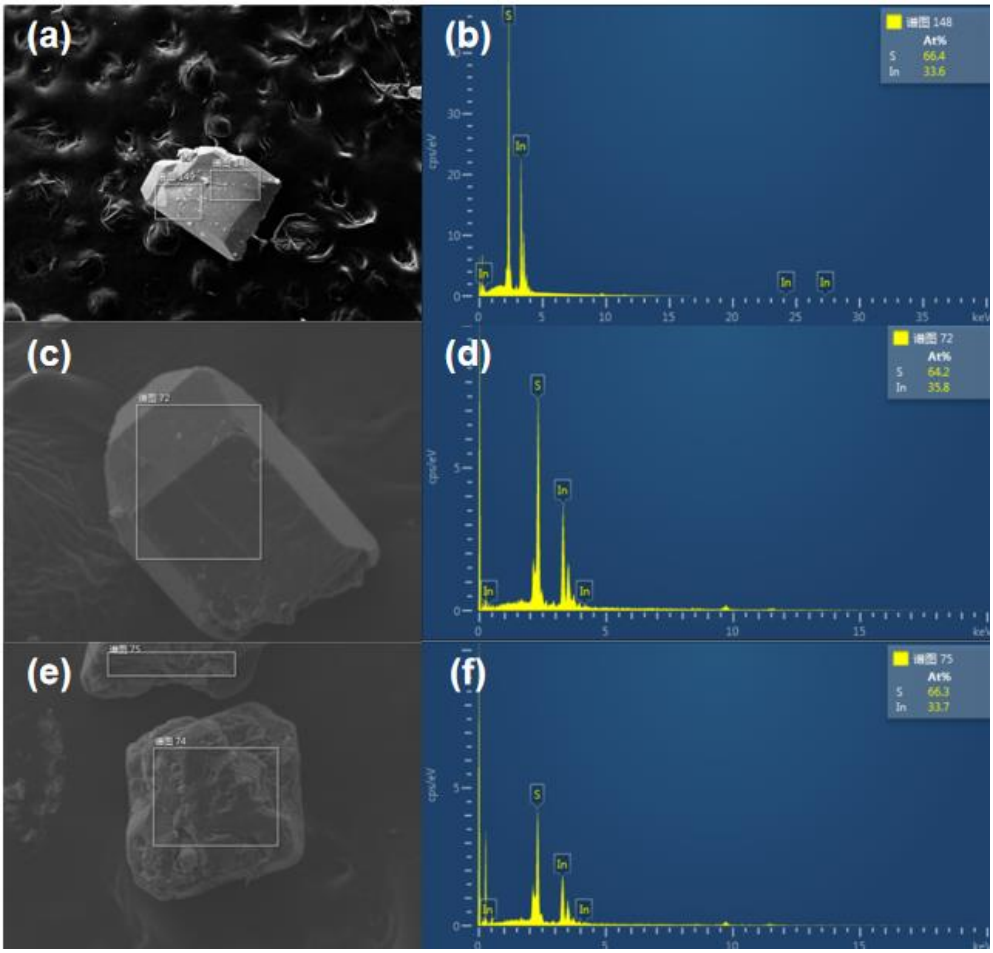

Fig. S18. SEM images (left) and EDS results (right) of **ISC-29** (a & b), **ISC-30** (c & d), and **ISC-31**(e & f).

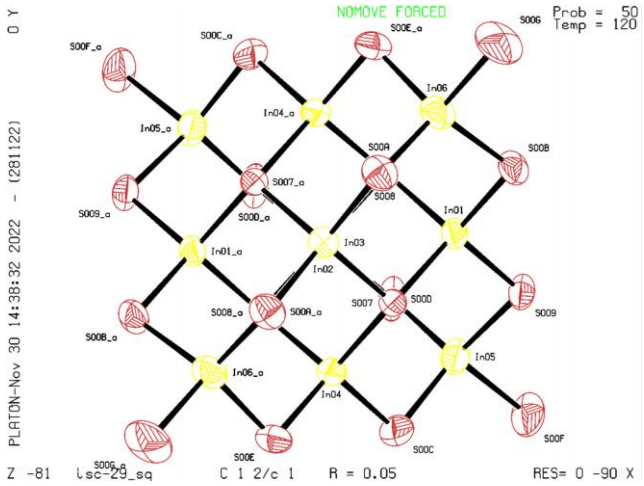

Fig. S19. ORTEP type model of **ISC-29** (T3-m).

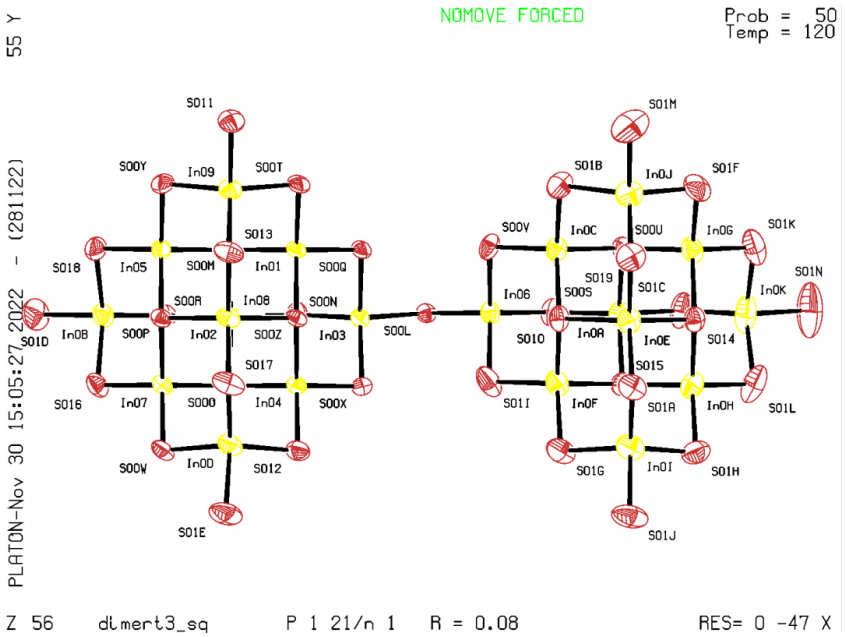

Fig. S20. ORTEP type model of **ISC-30** (T3-d).

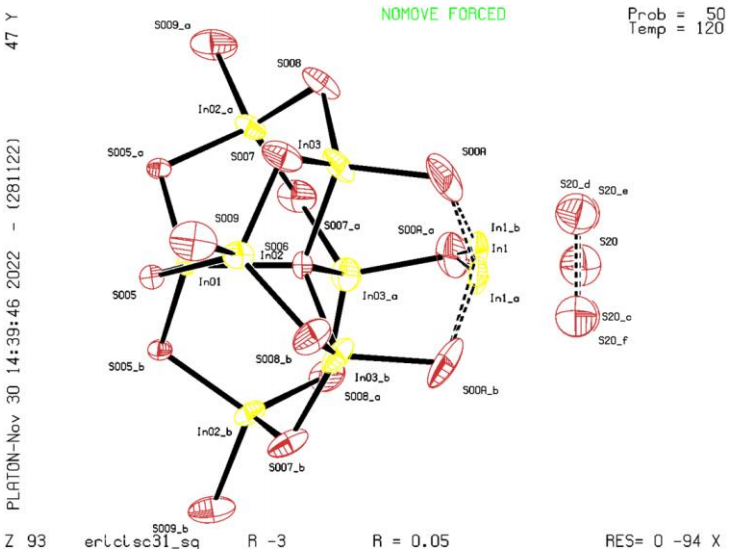

Fig. S21. ORTEP type model of **ISC-31** (P1-d).